An Improved Approach for Hybrid Rocket Injection System Design

M. Invigorito, G. Elia, M. Panelli

Abstract—Hybrid propulsion combines beneficial properties of both solid and liquid rockets, such as multiple restarts, throttability as well as simplicity and reduced costs. A nitrous oxide (N_2O)/paraffin-based hybrid rocket engine demonstrator is currently under development at the Italian Aerospace Research Center (CIRA) within the national research program HYPROB, funded by the Italian Ministry of Research. Nitrous oxide belongs to the class of self-pressurizing propellants that exhibit a high vapor pressure at standard ambient temperature. This peculiar feature makes those fluids very attractive for space rocket applications because it avoids the use of complex pressurization systems, leading to great benefits in terms of weight savings and reliability. To avoid feed-system-coupled instabilities, the phase change is required to occur through the injectors. In this regard, the oxidizer is stored in liquid condition while target chamber pressures are designed to lie below vapor pressure. The consequent cavitation and flash vaporization constitute a remarkably complex phenomenology that arises great modelling challenges. Thus, it is clear that the design of the injection system is fundamental for the full exploitation of hybrid rocket engine throttability. The Analytical Hierarchy Process has been used to select the injection architecture as best compromise among different design criteria such as functionality, technology innovation and cost. The impossibility to use engineering simplified relations for the dimensioning of the injectors led to the needs of applying a numerical approach based on OpenFOAM®. The numerical tool has been validated with selected experimental data from literature. Quantitative, as well as qualitative comparisons are performed in terms of mass flow rate and pressure drop across the injector for several operating conditions. The results show satisfactory agreement with the experimental data. Modeling assumptions, together with their impact on numerical predictions are discussed in the paper. Once assessed the reliability of the numerical tool, the injection plate has been designed and sized to guarantee the required amount of oxidizer in the combustion chamber and therefore to assure high combustion efficiency. To this purpose, the plate has been designed with multiple injectors whose number and diameter have been selected in order to reach the requested mass flow rate for the two operating conditions of maximum and minimum thrust. The overall design has been finally verified through three-dimensional computations in cavitating non-reacting conditions and it has been verified that the proposed design solution is able to guarantee the requested values of mass flow rates.

Keywords—Hybrid rocket, injection system design, OpenFOAM®, cavitation.

I. INTRODUCTION

THE development of hybrid propulsion systems based on hydrocarbons is becoming a technology asset for launchers and new generation space transportation systems. In particular, hybrid rocket engines based on LN_2O/Wax or LO_2/Wax, are good candidates for the future transportation systems since they combine advantages of both solid and liquid systems. Indeed, those systems use half of the plumbing of the liquid rockets but retain operation flexibility and low explosive hazard typical of solid rockets.

To this purpose, within the Italian national research program HYPROB, a specific project is dedicated to hybrid propulsion [1]. The objective is to increase the Technology Readiness Level (TRL) of this system through the development and test of a rocket engine demonstrator based on N_2O-Paraffin wax able to exploit and prove the throttability and re-ignition capabilities of hybrid rockets. The hybrid technological demonstrator is a pressure-fed 30 kN thrust class engine [2].

Nitrous oxide will be stored in liquid condition at room temperature and pressures of more than 5 MPa (its vapor pressure). In this way, the high density obtained turns into a smaller tank volume. During the feeding of nitrous oxide from the tank to the injection system, Fig. 1, the combustion chamber pressure will always be kept below its vapor pressure. This means that a phase change from liquid to vapor occurs along the feeding line, between the tank and the combustion chamber itself. In order to avoid an uncontrolled transition and mitigate feed system coupled instabilities, which could be detrimental and dangerous for stability reasons, forcing the phase change through the injector has been assumed as a design constraint. In this way, the oxidizer remains in the liquid condition until the injection head, whereas it will be gaseous at the injector exit. The consequent cavitation and flash vaporization is due to the expansion of the nitrous oxide along the injector at an almost constant temperature.

Further complications arise from the compelling requirement of thrust modularity. Indeed, the injection system must ensure the possibility of adjusting the mass flow to reduce the thrust down to the 30% of the nominal value.

M. Invigorito is with the Italian Aerospace Research Centre (CIRA), Via Maiorise snc, Capua, 81043 Italy (phone: +39 0823623097; fax: +39 0823623335; e-mail: m.invigorito@ cira.it).

G. Elia is with the Italian Aerospace Research Centre (CIRA), Via Maiorise snc, Capua, 81043 Italy (e-mail: g.elia@cira.it.).

M. Panelli is with the Methodologies and Technologies for Space Propulsion Department at the Italian Aerospace Research Centre (CIRA), Via Maiorise snc, Capua, 81043 Italy (e-mail: m.panelli@cira.it.).
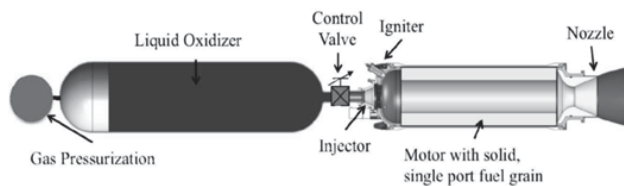
Fig. 1 Schematic of a typical pressure-fed hybrid rocket propulsion system

The complex phenomenology and the design requirements increase the importance of the injection system design phase and the choice of the injection architecture. For these reasons, the traditional design approach has been revised and in the following section the innovative elements will be discussed.

II. SCOPE OF THE CURRENT EFFORT

The scope of this effort is to improve the current design approach by investigating the applicability of innovative methods and numerical models to preliminary design the injection system of hybrid rocket engines.

Firstly, the injection system architecture, able to fulfill the design requirements, is presented as a result of a structured technique for organize and analyze complex decisions. Then, numerical tools and methods are explained. With the purpose of estimating the mass flow rate of the injection plate, multiphase CFD (Computational Fluid Dynamics) model are selected and validated using single injector elements. Finally, the consolidated numerical method is applied to the final geometry, closing the design loop.

III. INJECTION SYSTEM DESIGN

A. Selection of Injection System Architecture

For a hybrid rocket engine, the oxidizer mass flow rate is the only active control parameter for thrust modulation, thus the choice of the feeding system architecture, composed by the feeding line and the injector head subsystem, is a complex and impactful decision. This became even more important if the designer has the constraint to force the oxidizer phase transition through the injectors. The activity started with a wide literature survey to understand which are the possible architectural solutions able to satisfy, in principle, the requirements. Among all, five were selected and considered for the trade-off study.

The first solution is known as *Pintle Nozzle Technology*. This nozzle concept uses a fixed exit area and a mechanical pintle positioned in the nozzle throat region. The throat area, along with the expansion area ratio, is varied by axially moving this pintle. This leads to an increment in combustion chamber's pressure and the consequent increase in burning ratio and thrust. This concept has been used in solid rocket motors and tactical ballistic missiles and can be classified as a combustion efficiency control.

The second solution is the adoption of *Multi-Injector Plates*. The thrust modulation is obtained through the manual replacement of the injection plates that are characterized by different injection areas. This concept is based on keeping constant the injection pressure and thus it is not dependent on pressure regulators.

Another option is to adopt a system composed by a fixed injector head and a *Flow Control Valve* (FCV) positioned upstream in the feeding line. The oxidizer mass flow variation and the shut off are obtained through the control valve regulation. This architecture, called in the following *FCV-Fixed-Injector* has been widely used in the past and recent international missions for its intrinsically simplicity and low costs, [3]. It is worth to highlight that this concept implies an appropriate design of the injector head that has to guarantee good performances for each thrust regime.
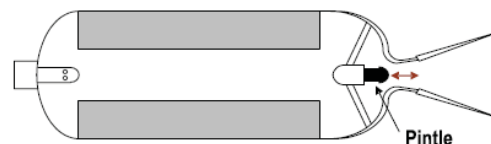

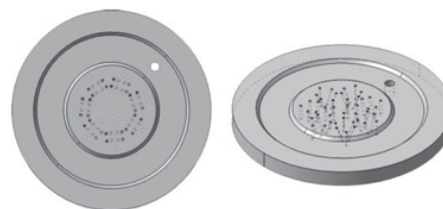
Fig. 2 Pintle nozzle sketch

Fig. 3 Top and isometric sketches of fixed-injector plate, [4]

Often used in liquid rocket engines, the *Pintle Injector* has unique features. In hybrids applications, an electromechanical actuated pintle is centered in the injection system just before the combustion chamber. The oxidizer flows around the pintle and is injected radially in the combustion chamber. Its axial position is easily linked to the injection area and thus the thrust control is accurate and rapid. Simple design, low combustion instabilities and high throttability make this concept very interesting, although high costs and strict requirements on manufacturing accuracy have to be taken into consideration [5].
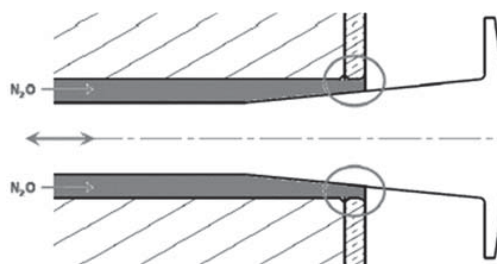

Fig. 4 Pintle injector sketch

In the final considered solution, the oxidizer mass flow modulation is obtained through the superimposition of a fixed perforated plate and a rotating injection plate. This solution, called *Rotating Plate*, allows modifying the injection area and the thrust by changing the relative position between plates. The

main advantage is the fast response to throttling and shut down whereas the manufacturing complexity and high costs are its main counterparts.

TABLE I
ANALYTIC HIERARCHY PROCESS TRADE OFF STUDY

Alternatives	Functionality					Technology		Cost	Total
	Throttability 33.4%	Reliability 6.3%	Stability 35.3%	Safety 14.8%	Efficiency 10.2%	Simplicity 75%	TRL 25%		
Pintle Nozzle Technology	0.012	0.002	0.010	0.005	0.003	0.008	0.030	0.010	0.079
Multi-Injector Plates	0.025	0.019	0.035	0.039	0.012	0.093	0.002	0.028	0.253
FCV + Fixed Injectors	**0.073**	**0.008**	**0.060**	**0.024**	**0.013**	**0.058**	**0.006**	**0.040**	**0.283**
Pintle Injector	0.067	0.008	0.097	0.017	0.026	0.021	0.011	0.022	0.269
Rotating Plate	0.035	0.004	0.021	0.009	0.010	0.015	0.017	0.006	0.116

The engine performance high sensitivity from this subsystem leads to the necessity of adopting a robust strategy for the decision making process. In this regard, the *Analytic Hierarchy Process* (AHP) has been chosen for its strong flexibility and effectiveness [6]. This tool is well suited when dealing with complex decision and aids to set priorities and make the best choice among several possible solutions. By reducing complex decision to a series of pairwise comparisons, and then synthesizing the results, the AHP helps to capture both subjective and objective aspects of a decision. In addition, the AHP incorporates a useful technique for checking the consistency of the decision maker's evaluations, thus reducing the bias in the decision making process.

Table I summarizes the results of the AHP methodology in terms of both, sub criteria weights and considered architectures scores. The hierarchic structure of the problem has been modeled considering three main criteria: functionality, technology innovation and costs. Some of those have been further detailed through the definition of sub criteria.

In particular, the functionality has been divided in *Throttability* that represents the easiness in modulating the thrust and the capability of having a wide range of thrust regime; *Reliability* of the overall architecture; *Stability* of the combustion process; *Safety* and combustion *Efficiency*. Moreover, the technological criterion has been split into *Simplicity* in terms of manufacturing easiness and *TRL improvement*. The AHP analysis revealed that the use of an architecture composed by an upstream flow control valve and a fixed injector head is the most appropriate solution. This option allows higher throttability variation if compared to the multi-injector plates solution and huge advantages in terms of simplicity and costs if compared to the pintle injector. This architecture has been selected and the design activity continued with the injection plate design [7].

B. Nitrous Oxide Propellant and Its Implications

Traditionally, modeling fluid dynamics in rocket propellant applications has been relatively straightforward due to the use of well-behaved fluids. Cryogenic oxygen, hydrogen peroxide and even cryogenic hydrogen are all modeled reasonably well using incompressible assumption even in their saturated state.

As well gaseous oxygen, hydrogen, helium and nitrogen are all fairly well modeled using the ideal gas assumption even in

the saturated state. For instance, the compressibility factor Z for saturated liquid cryogenic oxygen at atmospheric pressure is Z = 0.004 and even saturated oxygen vapor at cryogenic temperatures behaves fairly close to the ideal gas case with Z = 0.97. On the other hand, the compressibility factor of saturated liquid nitrous oxide at room temperature is Z = 0.13 and Z = 0.53 for saturated vapor, which makes the ideal gas and incompressible liquid assumptions inadequate for any kind of quantitative modeling as shown in Table II.

TABLE II
COMPRESSIBILITY FACTOR Z

Fluid	Z^L	Z^V
Water	0.000023	0.997
LOX (90K)	0.004	0.97
LH$_2$ (20K)	0.017	0.90
N$_2$O	0.13	0.53

Compressibility factor of common rocket propellants (and water) at their saturation states. LOX and LH$_2$ are saturated at 1 atm, others at 298 K.

Further insight on nitrous oxide behavior is shown in the P-ρ plane where the saturation curve and the 293 K isothermal line are presented, Fig. 5. It is clear that, assuming that nitrous oxide isothermally expands through the injector, going from liquid injection conditions (P ≈ 8.0 MPa) to chamber target pressure of about 4.0 MPa, the oxidizer experiences phase changes from liquid to vapor passing through the metastable region. Thus, in these operating conditions, the effects of compressibility are overshadowed by the introduction of two-phase flow. In these conditions, the well-known C_dA equation for the prediction of sub-cooled liquids flow rates of well-characterized injectors cannot be exploited, though it can still be used as a baseline for determining "effective" discharge coefficient. Furthermore, in cases where the bulk static pressure drops below the vapor pressure within the injector as shown in Fig. 5, significant vapor formation will occur, and the mass flow rate will be limited. This effect was demonstrated by the work of Hesson and Peck [9], in which the mass flow rate of saturated carbon dioxide (CO_2) through simple short orifices was studied (orifice length to diameter ratio L/D ~ 1.7). In this case, as the downstream pressure drops below this critical value, a maximum flow rate is achieved and preserved, essentially "choking" the orifice. This regime is referred to as *critical flow* as the mass flow rate

is independent of the downstream pressure. This physical behavior, peculiar of high vapor pressure propellants, such as nitrous oxide, can be exploited to perform throttling and thrust modulation within the hybrid rocket engines. Hence, it is possible to vary the mass flow rate simply through the regulation of the upstream pressure and independently from the combustion chamber pressure.
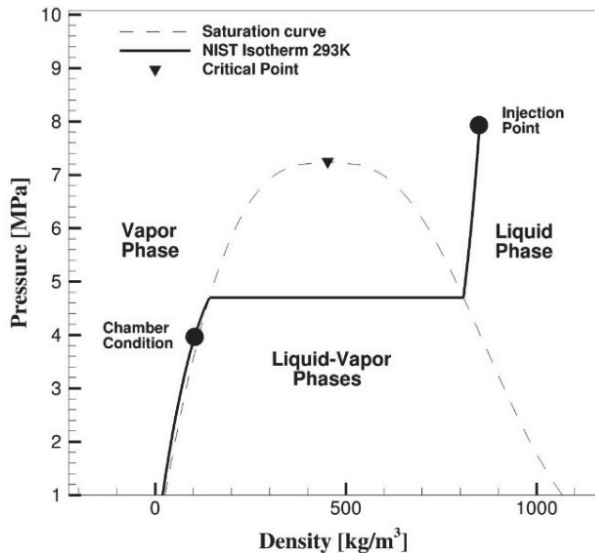

Fig. 5 $P - \rho$ diagram for nitrous oxide injection operation. Isotherm line at temperature of 293K. The data used to produce this plot was calculated using NIST database [8]

A variety of two-phase flow models attempt to account for the effects of two-phase flow as reported in [10], and do seem to capture the general mass flow rate behavior that should be expected. However, none of these models are in close agreement when it comes to the prediction of actual critical mass flow rate values over a wide range of operating conditions, and it is not obvious which models are the most accurate for application to hybrid rocket propellant where multiple injectors are needed.

C. Injection System Performance Requirements

The mass flow rates, associated to the required low and high thrust conditions of 10 kN and 30 kN, have been preliminarily evaluated using 0-D relations. Values of 4.65 kg/s and 10.9 kg/s have been obtained and taken as reference for the two thrust regimes. In particular, the global injection area has been calculated considering the low thrust operating condition, this is due to the possibility of increasing the mass flow rate, and thus the thrust, simply acting on the regulation valve. When the thrust is 10 kN, chamber pressure is 1.65 MPa. Those values have been used for the estimation, through two-phase models, of the necessary upstream pressure and total injection area. In particular, setting an upstream injection pressure of 5.5 MPa, an overall injection area of about 2.65e^{-4} m^2 has been determined. Then, it has been possible to evaluate the upstream pressure increase that guarantees a mass flow rate of 10.9 kg/s. This value, together with a combustion chamber pressure of 4.0

MPa, characterize the high thrust regime for the engine. Thus, keeping the overall injection area constant, a value of 7.5 MPa led to the achievement of 30 kN of thrust. Once known the overall injection area, the definition of the injection plate layout, in terms of number of injectors and their disposition, has been carried out by means of CFD simulations. The numerical tool, as shown in the next section, has been previously validated using literature data.

IV. VALIDATION OF THE NUMERICAL METHOD

Among available CFD codes, the OpenFOAM® multiphase solver, namely *interPhaseChangeFoam*, has been chosen for its capability to perform unsteady RANS simulations including appropriate models for phase change effects and interface tracking. The validation activity consists in assessing the reliability in terms of mass flow rate or pressure drop prediction with the purpose of using CFD to evaluate the required total area for the injection plate.
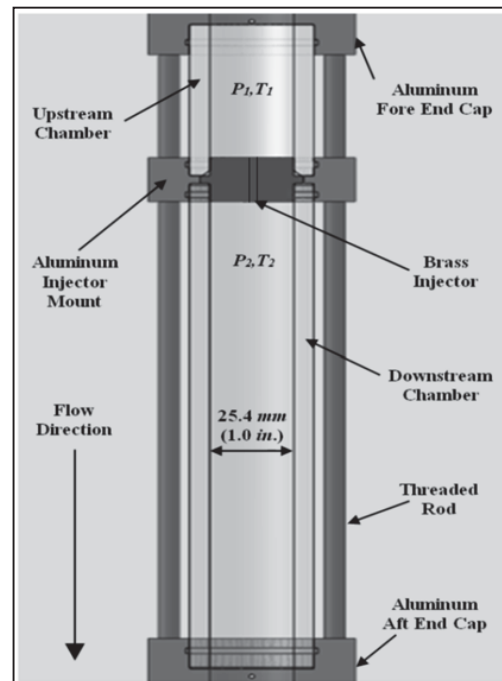

Fig. 6 Cross-section model for the test section of the experimental apparatus

A. Experimental Apparatus

The validation process presented in the following sections is based on the experimental cold flow testing campaign of Waxman, performed at the Stanford University [11]. The purpose of the experimental effort was to evaluate the performance of several injector designs at the operating backpressures observed during combustion testing. With this objective a test facility, capable to establish realistic values of operating upstream and downstream pressures, has been developed. In particular, the facility has been designed in such a way to easily change the injector plate assuring high testing flexibility. The test rig, shown in Fig. 6, is composed by

transparent polycarbonate tubes, closed on each end by aluminum end caps, to create a pressure vessel with optical access (internal diameter = 25.4 mm). In order to enable the test of a wide range of injector geometries, the injector insert was designed to be easily interchangeable. The brass insert, shown in Fig. 7, is mounted within an aluminum block that serves as junction between the upstream and downstream polycarbonate pressure vessels.

Fig. 7 Photo of the brass injector insert

The reference injector geometry is constituted by a plain orifice with an internal diameter D = 1.5 mm and length L = 18.42 mm. The cross-section is shown in Fig. 8.
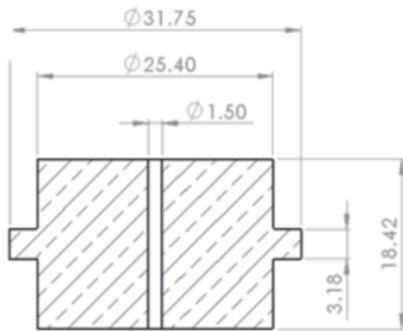

Fig. 8 Cross-section of the injector insert used as reference

Pressure and temperature are measured in both, upstream and downstream polycarbonate chambers, allowing the instantaneous measurement of ΔP and the determination of the upstream thermodynamic state.

B. Governing Equations

The *interPhaseChangeFoam* solver is based on the Volume of Fluid (VoF) [12] model and uses a mixture one-fluid approach. This solver solves the continuity and momentum equations, which are written for the mixture.

$$\frac{\partial \rho_m}{\partial t} + \nabla \cdot (\rho_m U) = 0 \qquad (1)$$

where U denotes the mixture velocity.

$$\frac{\partial \rho_m U}{\partial t} + \nabla \cdot (\rho_m UU) = -\nabla P + \nabla \cdot \left[\left(\mu_{eff}(\nabla U + (\nabla U)^T) \right) \right] + f_\sigma \qquad (2)$$

where μ_{eff} is the effective viscosity given by

$$\mu_{eff} = \mu_m + \mu_t. \qquad (3)$$

The mixture density and viscosity, respectively, are computed in *interPhaseChangeFoam* solver as

$$\rho_m = (1 - \alpha)\rho_v + \alpha \rho_l \qquad (4)$$

$$\mu_m = (1 - \alpha)\mu_v + \alpha \mu_l. \qquad (5)$$

The surface tension force is added to the momentum equation, and it is calculated per unit volume via *Continuum Surface Force* model as

$$f_\sigma = \sigma k \nabla \alpha \qquad (6)$$

where σ and α are the surface tension coefficient and the liquid volume fraction. The curvature k is defined as

$$k = -\nabla \left(\frac{\nabla \alpha}{|\nabla \alpha|} \right). \qquad (7)$$

In OpenFOAM®, an improved version of VoF technique, called *Compressive Interface Capturing Scheme for Arbitrary Meshes* [13], is implemented and used in the *interPhaseChangeFoam* solver. In this model an additional parameter, namely interface-compression velocity in the surrounding of the interface is described to promote the interface resolution by steepening the gradient of the volume fraction function, which is represented in the transport equation for α shown below.

$$\frac{\partial (\alpha \rho_l)}{\partial t} + \nabla \cdot (\alpha \rho_l U) + \nabla \cdot [\alpha U_c (1 - \alpha)] = R_c - R_e \qquad (8)$$

where R_e and R_c denote the rate of mass transfer for evaporation and condensation, respectively. Cavitation models accuracy correspond to the correct representation of these source terms and within the solver framework three cavitation model are already implemented. These are Merkle [14], Kunz [15] and SchnerrSauer [16].

The term in the square bracket represents the artificial compression term and it describes the shrinkage of the phase-interphase towards a sharper one as it defines the flow of α in the normal direction to the interface [17].

$$U_c = min[C_\alpha |U|, max(|U|)] \frac{\nabla \alpha}{|\nabla \alpha|} \qquad (9)$$

An iterative PIMPLE algorithm coupled with α-phase sub-cycle is employed to solve pressure-velocity coupling and achieve continuity. Further detail about the algorithm and the VoF method implemented is given in [18].

C. Computational Domain and Boundary Conditions

For the investigation and validation of the numerical method, considering the specific application, the injector-like geometry of Waxman is considered. Since this geometry is symmetric, only half of the geometry is calculated using a two-dimensional axisymmetric computational domain, shown in Fig. 9.

The results of the CFD calculation are known to be affected by the resolution of the computational mesh, especially in the regions of high gradients. In order to verify the grid

independence of the solution, different refinements have been performed. Due to pressure and velocity gradients, the mesh is refined at the inlet corner and in the upper part of the nozzle.

However, in terms of injection rates, the differences between the meshes are not significant, while the local refinement at the nozzle entry is needed to capture the large pressure and velocity gradients in this region related with the onset of cavitation, as stated in [19]. The final chosen mesh is made of a structured grid of 20460 hexahedral cells. In order to perform numerical simulations and validate the multiphase solver for our specific application, the operating conditions have been chosen among the experimental data available in [11].
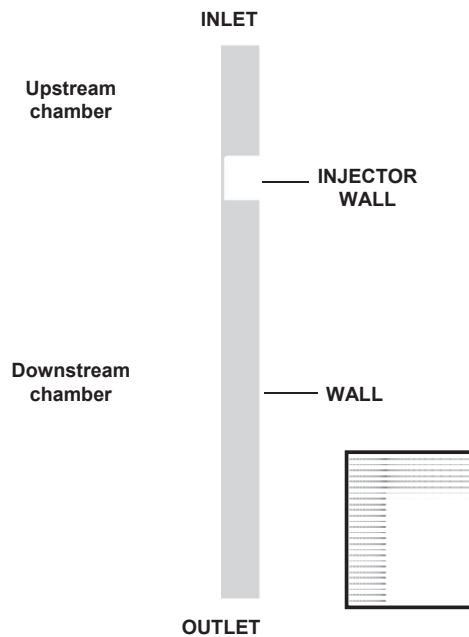

Fig. 9 Schematic of 2D computational domain and boundary conditions. Particular of mesh at injector entrance

TABLE III
TEST MATRIX TM1

Case	A	B	C	D
$\Delta P\ [MPa]$	1.5	2.5	3.5	4.5
$P_2\ [MPa]$	5.43	4.43	3.43	2.43

Injection conditions: inlet pressure P1 = 6.93 MPa, inlet temperature T1 = 283 K; and vapor pressure: Ps= 4.02 MPa.

TABLE IV
TEST MATRIX TM2

Case	A	B	C
$\Delta P\ [MPa]$	3.5	3.0	3.0
$P_1\ [MPa]$	7.05	6.10	5.3
$P_2\ [MPa]$	3.55	3.10	2.30
$\dot{m}\ [kg/s]$	0.100	0.080	0.065

Injection temperature: T1 = 283 K; vapor pressure: Ps= 4.02 MPa.

Consequently, two simulation strategies have been defined and resulted in test matrices TM1 and TM2 whose operating points are listed in Tables III and IV.

The main objective of test matrix TM1 is the investigation of the onset of cavitation and its consequence on mass flow rate prediction, by imposing injection pressure and varying pressure drop across the injector. Furthermore, the test matrix TM2 is defined with the purpose of evaluating the selected multiphase solver for the specific application: critical mass flow rate at different injection pressure and equivalently, for the same mass flow, the pressure drop across the injector are evaluated and compared with respect to the experimental values. In TM2, two strategies have been adopted. In the first case, the pressure inlet and pressure outlet have been fixed, while in the second case the fixed boundary conditions have been the inlet mass flow rate and the pressure outlet. In each case, the non-slip wall boundary condition has been assumed.

In the experiment as well as in the numerical calculations, nitrous oxide is used as fluid, whose thermodynamic and transport properties are derived from the NIST database, [8]. The flow inside the injector can be reasonably considered turbulent since its Reynolds number is about 60000. Hence, a turbulence model is required for the simulations and, considering the results obtained in [20], k-Omega SST turbulence model is used in combination with the automatic wall treatment which ensures flexibility for y+ value at walls.

D. Computational Strategy

The multiphase solver is based on the finite volume approach and the iterative process is performed by the PISO algorithm, [21]. Although the inlet and outlet boundary conditions are imposed and constant in time, the modeling of the cavitation phenomenon itself is transient. Hence, the cavitating flow is calculated in a time marching manner, even if the final solution is steady state. In order to accelerate the convergence and ensure stability, the solution is initialized opportunely by filling the first three-fourth of the injector with the fluid at liquid condition.

The solution is obtained using an average integration time step of 0.1 µs over 300,000 time-steps to simulate at least two or three injector flow-through times, this amounts to approximately 30 ms of injector operation.

Each simulation ran on 16 processors consuming about 96 CPU hours on a core of Intel Xeon E5 64 bit at a clock frequency of 2.7 Ghz. All numerical computations have been performed by using second-order accurate numerical scheme in space.

E. Validation Results

The experimental characterization of plain orifice injector carried out in [11] has been used in this work as a reference to validate the CFD models. In the experiments, the injection pressure has been kept constant, while backpressure has been varied to get the corresponding pressure drop, and thus study the mass flow rate in non-cavitating and cavitating conditions.

1. Cavitation Behavior

In Fig. 9, the results, in terms of injection mass flow rate, achieved within the test matrix TM1 (Table III) at different pressure drops and fixed injection pressure are compared with the experimental measurements. The study aims to show the

ability of the model to accurately predict the injector mass flow at different cavitating conditions and give further insight to cavitation behavior of nitrous oxide.
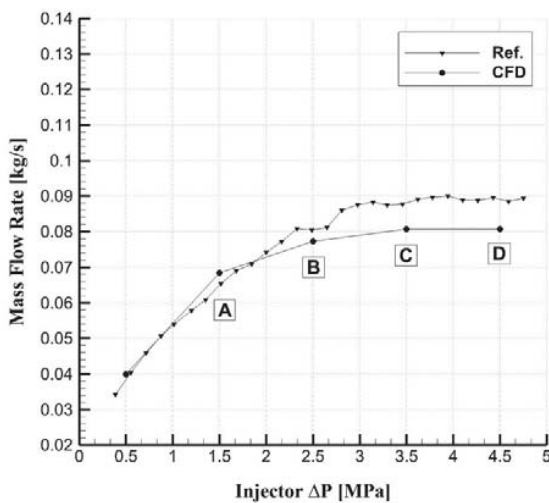

Fig. 9 Mass flow rate vs. ΔP at fixed injection pressure for injector with nitrous oxide. P1 = 6.93 MPa, T1 = 283 K; Ps= 4.02 MPa
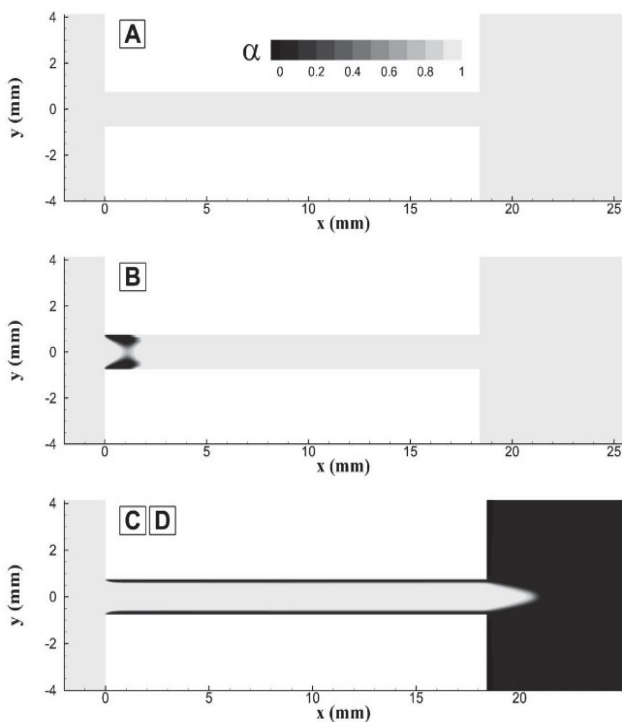

Fig. 10 Liquid volume fraction distributions: (a) non cavitating; (b) incipient cavitation; (c) and (d) cavitation with choking.

In Fig. 9, the injection rate, expressed in kg/s, is reported as a function of pressure drop across the injector for fixed temperature and thus vapor pressure. The deviation of simulation results from the experimental data occurs with the onset of the cavitating condition, shown in Fig. 10 B. The error

in mass flow prediction increases in magnitude up to the establishment of choked cavitating condition. From this point, an increase in pressure drop does not affect the model accuracy in terms of mass flow prediction, see Table V. The numerical model is able to capture the independence of mass flow from changes in pressure drop in choked regime with satisfactory degree of confidence. In the liquid volume fraction contours of injection flow fields depict the evolution of physical phenomenon associated with pressure drop increase. As a matter of fact, starting from lower pressure drop, for which liquid condition is dominant (Fig. 10 A), backpressure raises lead to cavitation inception (Fig. 10 B) and subsequent developed cavitation zone with steep phase change at injector exit (Fig. 10 C and D).

Results from test matrix TM1 are extremely useful in the first characterization of nitrous oxide injector mass flow rate performance. Furthermore, these simulations give useful insights about the behavior of nitrous oxide injectors operating in the two-phase flow regime.

TABLE V
TEST MATRIX TM1

	A	B	C	D
$\dot{m}$ error	+5.3%	-4.1%	-8.3%	-9.2%

Error in mass flow prediction for test matrix A with respect to experimental data. Injection conditions: inlet pressure P1 = 6.93 MPa, inlet temperature T1 = 283 K; and vapor pressure: Ps= 4.02 MPa.

2. Injection Rate Prediction

With the Test Matrix TM2, shown in Table IV, the accuracy of the two-phase flow solver previously described is evaluated, even though more experimental cold flow data would be required to make a definitive ranking of the model performance. However, at this point, it is still useful to increase confidence in the mass flow rate performance and predictions of a given injector geometry and operating conditions using these cold flow test data like the one presented below. With this purpose in mind looking at the experimental data, shown in Fig. 11, the three selected operating points are investigated by the OpenFOAM multiphase solver interPhaseChangeFoam. These three operating points are chosen since they lay completely inside the choked injection regime, as this condition is the most relevant for our application due to the independence of the injection rate from the chamber pressure.

Fig. 12 compares the predicted mass flow rate obtained by the selected multiphase solver vs. the experimental mass flow rate. For each experimental test data, a prediction of the critical mass flow rate is calculated with the multiphase solver and the corresponding individual points are plotted. This is done for tests in TM2. In order to assess the accuracy of the given solver, a series of straight lines are included in the plot, corresponding to different levels of error in the critical flow rate predictions (continuous lines correspond to ±20% error and dashed lines to ±15% error).
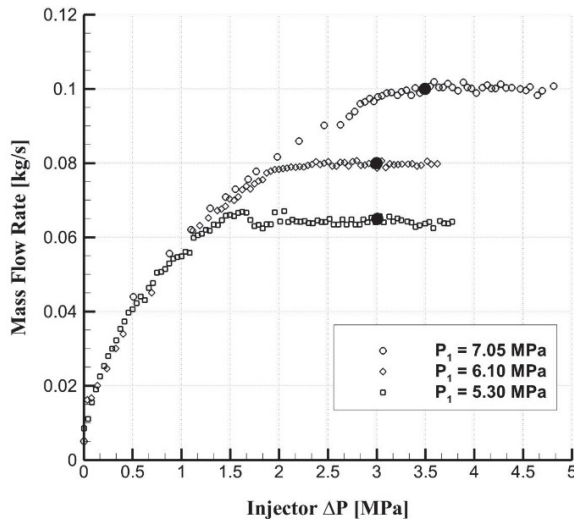
Fig. 11 Experimental data for mass flow rate vs. ΔP at different fixed injection pressures for injector with nitrous oxide. P1 [5.30, 6.10, 7.05] MPa, T1 = 283 K; Ps= 4.02 MPa. Red circles, operating points of *TM2*
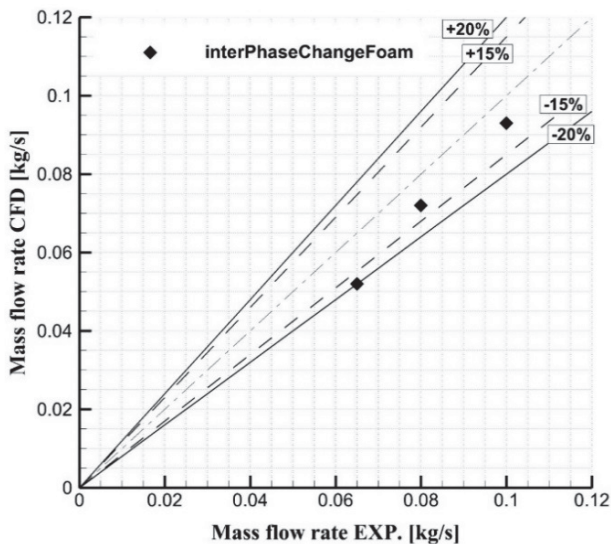

Fig. 12 Comparison of experimental critical mass flow rate data to that predicted by the multiphase solvers. (Continuous lines correspond to ±20% error, dashed lines to ±15% error)

TABLE VI
MASS FLOW RATE PREDICTION ACCURACY

Exp. [kg/s]	interPhaseChangeFoam [kg/s]	ERROR %
0.065	0.052	-20.00
0.080	0.072	-9.75
0.100	0.093	-7.10

Injection temperature: T_1 = 283 K; vapor pressure: P_s= 4.02 MPa

From examining Fig. 12 and results reported in Table VI, it can be seen that the solver tends to underestimate the mass flow rate over the entire set of data. This is expected because the

model employed represents a lower bound on the two-phase mass flow rate, as seen from test matrix TM1.

Increasing injection rates the solver present a tendency to reduce its error with respect to the experimental data, but it is difficult to establish if this tendency is deterministic due to the lack of experimental data in the low flow rate region.

3. Pressure Drop Prediction

Fig. 13 compares the predicted pressure drop across the injector calculated by the selected multiphase solver vs. the experimental measured value. For each experimental test dataset, a prediction of the ΔP is calculated and the corresponding individual points are plotted. This is repeated for tests in TM2.

In order to assess the accuracy of interPhaseChangeFoam, a series of lines are included in the plot, corresponding to different levels of error in the critical pressure drop predictions (continuous lines correspond to ±20% error and dashed lines to ±15% error). From examining Fig. 13 and results reported in Table VII, it can be seen that the solver tends to overestimate the pressure drop across the injector over the entire set of data. This is expected because the model employed represents a lower bound on the two-phase mass flow rate and as a consequence this behavior is reflected in increased pressure when experimental injection rate is imposed.
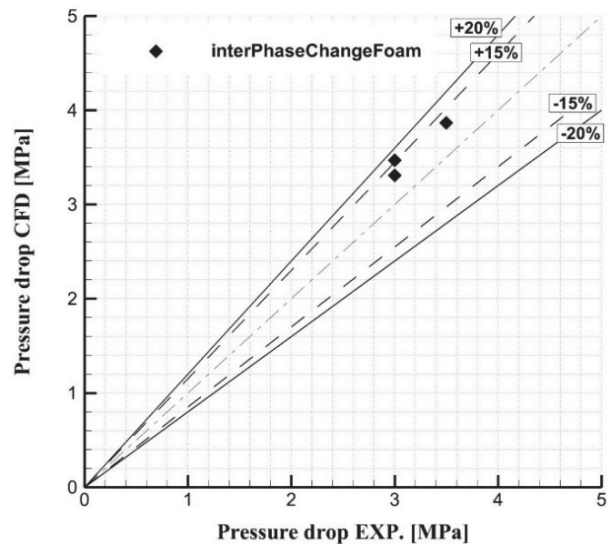

Fig. 13 Comparison of experimental critical pressure drop data to that predicted by the multiphase solvers. (Purple lines correspond to ±20% error, green lines to ±15% error)

TABLE VII
INJECTOR PRESSURE DROP PREDICTION ACCURACY

Exp. [MPa]	interPhaseChangeFoam [MPa]	ERROR %
3.000	3.468	15.60
3.000	3.310	10.33
3.500	3.865	10.43

Injection temperature: T_1 = 283 K; vapor pressure: P_s= 4.02 MPa

V. INJECTION PLATE DEFINITION

The quality and homogeneity of an atomized fluid, and therefore the stability and combustion efficiency of hybrid rocket engines, are basically determined by the injection system. In order to choose an optimal solution, different configurations, available in literature, have been considered and compared. The final choice has been done referring to an experimental campaign conducted on four different injection plate layouts and which results are reported in [4]. Being the mass flow rates of the demonstrator different from the one of the study, the only features adopted have been the number of injectors and a similar, but not identical, spatial distribution. In Fig. 14, the sketch of the injection plate is shown.
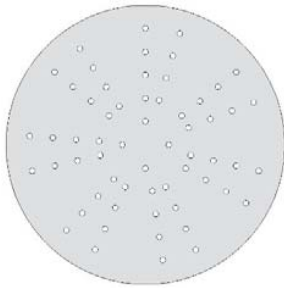

Fig. 14 2D scheme of injectors distribution

The 60 axial injectors are distributed on five circles with an offset of 10 mm each. In particular, the first circle is composed by 4 injectors while 14 injectors constitute the others.

Once the number of injectors is defined, knowing the total injection area, it has been possible to evaluate and verify through CFD simulations that an injector diameter of 2.4 mm guarantee the oxidizer mass flow rate associated to the low thrust condition. Furthermore, in order to have a fully developed flow inside the injector, an aspect ratio of 7.5 has been chosen, resulting in a total injector length of 18 mm. It's of utmost importance to highlight that those geometrical characteristics are not problematic in terms of manufacturability.

VI. INJECTION PLATE VERIFICATION

Using an increasing complexity strategy, an extensive CFD matrix has been defined. Simulations have been performed for a single injector, firstly, then for the entire 3D injection plate geometry, considering the coupling with the combustion chamber and both thrust regimes.

In particular, the complete 3D geometry exploited the possible symmetry hypothesis of the injection plate and thus the computational domain was reduced to a wedge of about 51 degrees resulting in an unstructured mesh of about 900000 cells. A detail of the unstructured mesh is reported in Fig. 15.

For turbulence closure, the Menter SST k-omega turbulence model has been used for its essential feature of accurate and robust near-wall treatment. Moreover, all numerical computations have been performed using second-order accurate numerical schemes in space.
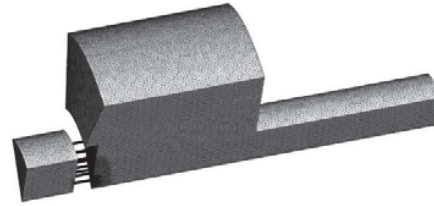

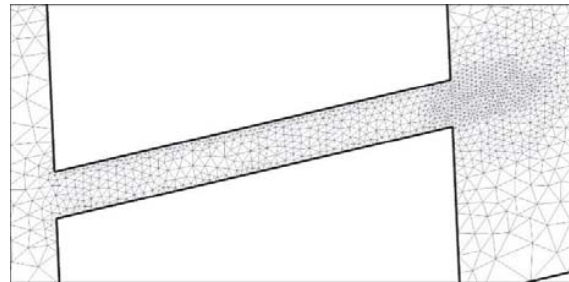Fig. 15 Injection chamber, injection plate and pre combustion chamber: tetrahedral mesh

Fig. 16 Detail of injectors' mesh

Two calculations, obtained imposing the values of inlet-outlet pressures related to the higher and lower thrust regime are reported (7.5-4.0 MPa and 5.5-1.65 MPa).

The comparison between the contours of velocity magnitude in a section (A-A) of the computational domain, cutting four injectors, reveals similar distributions, with gas expansion near the injectors' exits and a significant recirculating flow in the pre-combustion chamber Fig. 17.

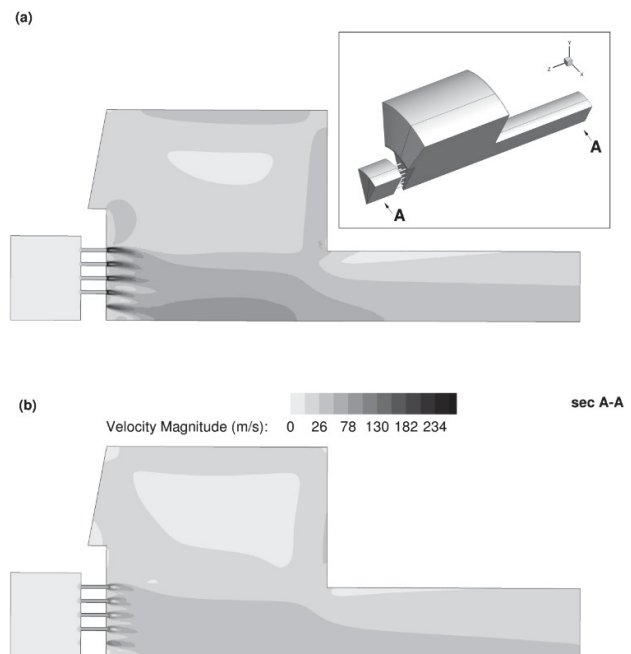Velocity Magnitude (m/s): 0 26 78 130 182 234

Fig. 17 Sec A-A: Contour of velocity magnitude: (a) 5.5-1.65 MPa, (b) 7.5-4.0 MPa up/downstream pressure

Despite qualitative similarity, the field differs in terms of absolute values. It is worth to notice that the average absolute velocity magnitude in low thrust test case is considerably higher than the one obtained for the high thrust regime. This occurs because, for the high thrust regime, even if the total mass flow rate increases, the density is higher and thus the average velocity magnitude is lower.
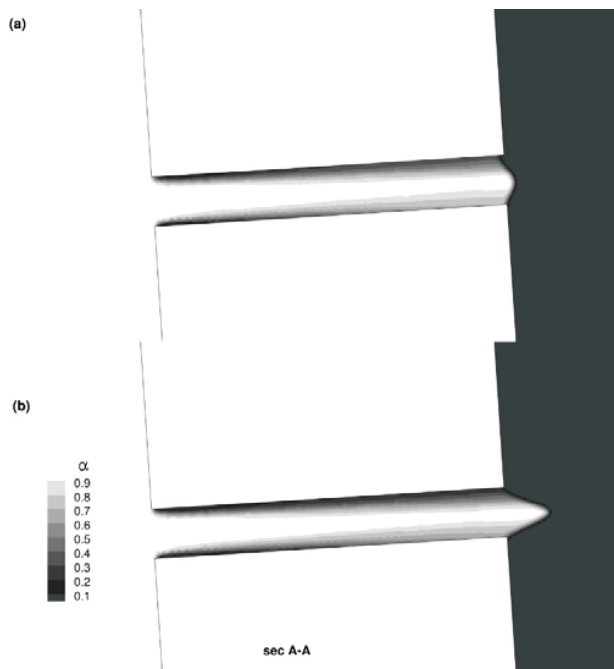

Fig. 18 Liquid volume fraction distributions: cavitation with choking in the 3D injection plate simulation. Inlet-outlet pressure (a) 5.5-1.65; (b) 7.5-4.0 MPa

The cavitation occurred for both thrust regimes; however, as it can be denoted from Fig. 18, different exit profiles of the liquid volume fraction are developed.

The simulations verified that, increasing the upstream pressure from 5.5 to 7.5 MPa the total mass flow rate increases from about 4.8 kg/s to 11.5 kg/s, with an error of less than 6% if compared to the hypothesized values of 4.65 and 10.9 kg/s. These results will be further refined with the reacting flow simulations in the next phase of the project. The simulation campaign assessed the feasibility of throttle the engine simply varying the injection pressure through the flow control valve.

VII. CONCLUSION

An improved design process, combining theoretical and numerical approach, has been presented and applied.

The injection system architecture composed by a fixed injection head and a flow control valve has been selected as the result of an AHP study to fulfill project requirements.

Modeling challenges have been identified and a numerical tool has been identified and validated against representative experimental data.

The injection plate has been preliminary designed with 60 injectors whose diameter has been selected in order to reach the requested mass flow rate for the two operating conditions of maximum and minimum thrust. Then, three-dimensional computations in cavitating non-reacting conditions verified that the design solution is able to guarantee the required performances.

It was found that the interPhaseChangeFoam solver could reasonably predict the main features of the flow field linked to the presence of cavitation through the nozzle. While it is clear that this multiphase solver is accurate enough in predicting the critical mass flow rates and pressure drop in the 0.1 kg/s mass flow region, it is not yet possible to definitively assure its accuracy in a wider range of operating conditions. More experimental data in both low and high injection rate regions would certainly be required to make such a definitive conclusion.

The demonstrated error levels shown for the interPhaseChangeFoam solver are promising, indeed, this model predict critical mass flow rates and pressure drop within 10% of the experimental values over the majority of the tests reported in this work. Further consideration could be done to justify the error level revealed by the simulations, but the tendency to underestimate the mass flow rate is conservative. As a matter of fact, it introduces a safe margin in designing injection system since it guarantees that desired thrust level is achieved.

REFERENCES

[1] S. Borrelli et al., "The HYPROB Program Mastering Key Technologies, Design and Testing Capabilities for Space Transportation Rocket Propulsion Evolution" in *Proc. 63rd International Astronautical Congress*, Naples, Italy, 2012.

[2] M. Di Clemente et al., "Hybrid rocket technology in the frame of the italian HYPROB program" in *Proc. 8th European Symposium on Aerothermodynamics and Space Vehicles*, Lisbon, Portugal, 2015.

[3] P. Dvorak, R. Tijsterman, "Numerical and experimental evaluation of the performance of a cavitating valve for the control of oxidizer flow in a hybrid rocket engine" in *Proc. 5th European Conference for Aeronautics and Space Sciences, EUCASS*, Munich, Germany, 2013.

[4] E. Gamper et al., "Design and test of nitrous oxide injectors for a hybrid rocket engine", in *Proc. Deutscher Luft- und Raumfahrtkongress*, Stuttgart, Germany, 2013.

[5] G. A. Dressler, J. M. Bauer, "TRW pintle engine heritage and performance characteristics", in *Proc. 36th Joint Propulsion Conference and Exhibit*, Huntsville, USA, 2000.

[6] T.L. Saaty, *The Analytic Hierarchy Process*. New York, NY: McGraw-Hill, 1980.

[7] G. Elia, et al., "Injection system design of an N_2O-Paraffin hybrid rocket demonstrator" in *Proc. 3rd ECCOMAS YIC*, Aachen, Germany, July 20-23, 2015.

[8] P. J. Linstrom and W. G. Mallard, editors. NIST Chemistry WebBook, NIST Standard Reference Database Number 69. National Institute of Standards and Technology, Gaithersburg MD, 20899, June 2005.

[9] J. Hesson and R. Peck, "Flow of two-phase carbon dioxide through orifices," *AIChE Journal*, vol. 4, issue 2, pages 207–210, 1958.

[10] J. Dyer, E. Doran et al., "Modeling feed system flow physics for self-pressurizing propellants", in *Proc. 43rd AIAA/ASME/SAE/ASEE Joint Propulsion Conference and Exhibit*, Cincinnati, OH, USA, 2007.

[11] B.S. Waxman, "An investigation of injectors for use with high vapor pressure propellants with applications to hybrid rockets", PhD Thesis. Stanford University, 2014.

[12] C.W. Hirt and B.D. Nichols, "Volume of fluid method (VOF) for the dynamics of free boundaries", *Journal of Computational Physics*, vol. 39, issue 1, pages 201-225, 1981.

[13] O. Ubbink, "Numerical prediction of two fluid systems with sharp interfaces", PhD Thesis, University of London, 1997.

[14] C.L. Merkle et al., "Computational modeling of the dynamics of sheet cavitation", in *Proc. 3rd International Symposium on Cavitation*, pages 47-54, Grenoble, France, 1998.

[15] R.F. Kunz et al., "A preconditioned Navier-Stokes method for two-phase flows with application to cavitation prediction", *Computer and Fluids*, vol. 29, issue 8, pages 849-875, 2000.

[16] G. Schnerr and J. Sauer, "Physical and numerical modeling of unsteady cavitation dynamics", in *Proc. 4th International Conference on Multiphase Flow*, New Orleans, USA, 2001.

[17] H. Weller, "A new approach to VOF-based interface capturing methods for incompressible and compressible flow". Report TR/HGW/04. OpenCFD Ltd., 2008.

[18] S.S. Deshpande et al., "Evaluating the performance of the two-phase flow solver interfoam", *Computational Science and Discovery,* vol. 5, Issue 1, 2012.

[19] X. Margot et al., "Numerical modeling of cavitation: validation and parametric studies", *Engineering Application of Computational Fluid Mechanics*, vol. 6, issue 1, pages 15-24, 2012.

[20] M. Invigorito et al., "Application of OpenFOAM for rocket design", in *Proc. 9th OpenFOAM Workshop,* Zagreb, Croatia, 2014.

[21] R.I Issa, "Solution of the implicitly discretized fluid flow equations by operator-splitting", *Journal of Computational Physics*, vol. 62, issue 1, pages 40-65, 1986.